Gary S. Was

# Fundamentals of Radiation Materials Science

## Metals and Alloys

With 381 Figures

Springer

Gary S. Was
Nuclear Engineering and Radiological Sciences
Materials Science and Engineering
University of Michigan
1921 Cooley Bldg.
2355 Bonisteel Blvd.
Ann Arbor, MI 48109-2104, USA
e-mail: gsw@umich.edu



Library of Congress Control Number: 2007922926

ISBN 978-3-540-49471-3 Springer Berlin Heidelberg New York



Springer is a part of Springer Science+Business Media

springer.com



Typesetting and production: LE-TEX Jelonek, Schmidt & Vöckler GbR, Leipzig
Cover design: eStudio Calamar S.L., F. Steinen-Broo, Girona, Spain

Printed on acid-free paper 54/3180/YL – 5 4 3 2 1 0

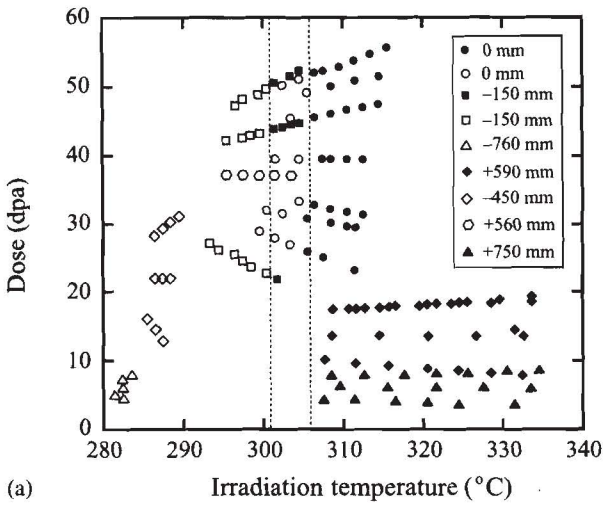


(a)

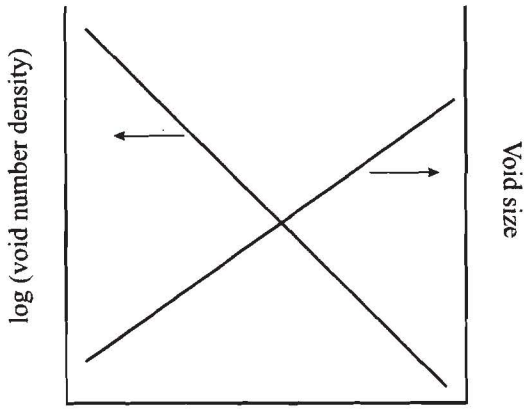


(b)

**Fig. 8.18.** (a) Dose-temperature plot of swelling in a Fe–Cr–Ni alloy irradiated in the BN-350 fast reactor showing the sharp temperature threshold for swelling (after [18]). (b) Schematic of the temperature dependence of void density and void size

eral behavior of the void number density and size with temperature is shown in Fig. 8.18b. With increasing temperature, the void density falls logarithmically and the size increases, which is the typical behavior for a process that is dominated by nucleation at low temperatures where the void growth is slow, and by growth at high temperature where the free energy difference driving void growth is small.

Figure 8.19 shows images of the microstructure in a baffle bolt used to secure baffle former plates against the baffle in a pressurized water reactor. In this case, the head was closest to the core (received the highest dose), and was exposed to the coolant, hence the lowest temperature. Gamma heating caused the temperature to exceed the coolant temperature (~ 320 °C) along the length of the bolt. While the

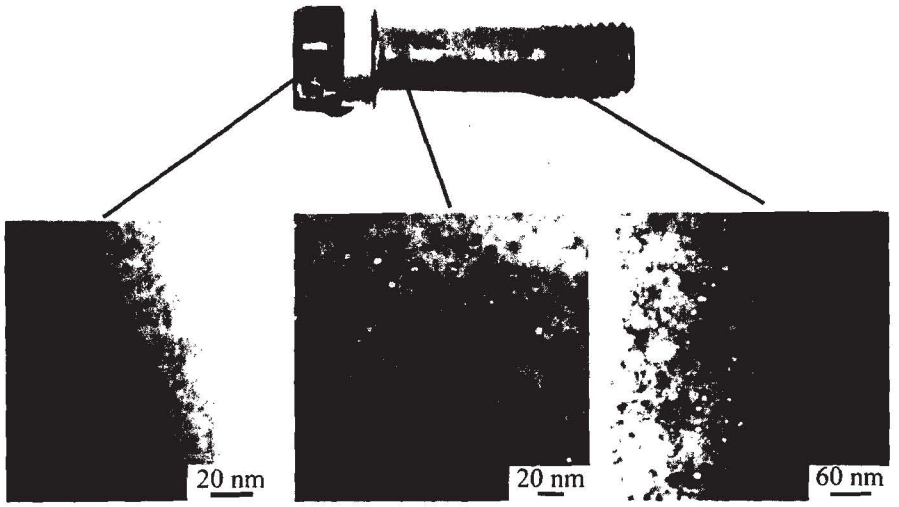


**Bolt Head, 0 mm**
**19.5 dpa, ~320°C**

**Top Shank, 25 mm**
**12.2 dpa, ~340°C**

**Near Threads, 55 mm**
**7.5 dpa, ~330°C**

**Fig. 8.19.** Swelling in a cold-worked 316 SS baffle bolt in a PWR as a function of position along the bolt length. The bolt head was closest to the core and the temperature distribution is caused by a combination of gamma heating and whether the bolt was exposed to the coolant (courtesy S.M. Bruemmer and Garner FA, PNNL)

doses differ somewhat, the dominant influence of temperature is noted by both the lack of voids in the lowest temperature location (head) and the largest void size at the highest temperature (top shank).

### 8.3.2 Dose Dependence

Understanding how swelling depends on dose is critical in the design and operation of components in radiation environments in which voids have the potential to form and grow. From the discussion in the previous section, the dependence is complicated by the occurrence of the defect production rate, $K_0$, in the terms $\dot{R}_0$ and $F(\eta)$. So we will take a different approach in determining the void growth rate dependence on dose, following that of Mansur [5]. Recall the expressions for $C_v$ and $C_i$ given in Eq. (8.119):

$$C_v = \frac{D_i k_i^2}{2K_{iv}} \left[ (\eta + 1)^{1/2} - 1 \right]$$

$$C_i = \frac{D_v k_v^2}{2K_{iv}} \left[ (\eta + 1)^{1/2} - 1 \right] ,$$

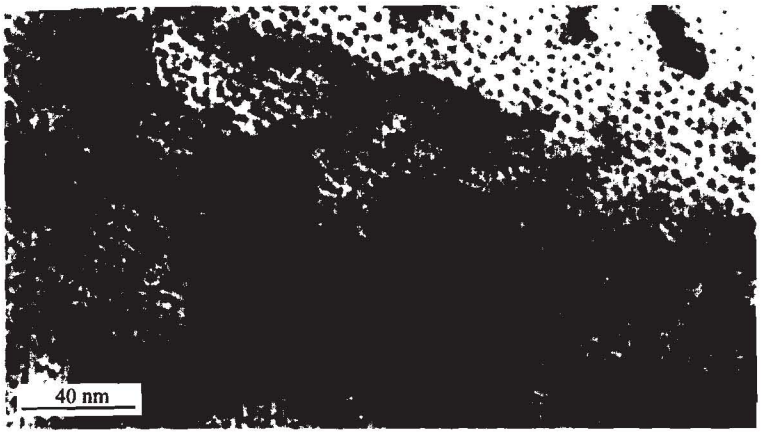


**Fig. 8.54.** He gas bubble superlattice formed in molybdenum following 40 keV $He^+$ irradiation to a dose of $5 \times 10^{21}$ $He^+/m^2$ at 500 °C (after [39])

### 8.4.5 Helium Production

An important ingredient in bubble formation and growth is the production of helium. In a reactor, He production is governed by the boron and nickel contents of the alloy through the reactions:

$$^{10}B(n,\alpha)^7Li\,, \tag{8.227}$$

and the two-step reaction:

$$^{58}Ni(n,\gamma)^{59}Ni(n,\alpha)^{56}Fe\,. \tag{8.228}$$

The thermal neutron $(n,\alpha)$ cross section for $^{10}B$ is very large, about 3837b, while the cross section for $^{59}Ni$ is for fast neutrons and is only about 4.3b. For thermal reactors then, a large amount of helium is produced early in life from transmutation of boron, but this source burns out by about 1 dpa ($\sim 10^{21}$ n/cm$^2$). The presence of nickel in stainless steels provides a smaller but sustained source of helium at higher dose. In this regard, thermal reactors produce greater amounts of helium at low dose and in a lower dose rate environment, making low dose helium-induced swelling a greater problem in a thermal reactor than in a fast reactor. Figure 8.55 shows the production rate of helium from an alloy containing $^{58}Ni$ and $^{10}B$ in the HFIR (thermal) reactor. Note that the production rate of helium is dominated at low fluence by the contribution from $^{10}B$, and at higher fluence by $^{58}Ni$. Helium buildup for the same alloy in a fast reactor and a fusion reactor are shown for comparison. Note that the helium buildup in a fusion reactor matches that in HFIR, and both are higher than that in a fast reactor.

# 15 Environmentally Assisted Cracking of Irradiated Metals and Alloys

A growing concern for electric power utilities worldwide has been the degradation of core components in nuclear power reactors, which provide approximately 17% of the world's electric power production. Service failures have occurred in boiling water reactor (BWR) core components and, to a somewhat lesser extent, in pressurized water reactor (PWR) core components consisting of iron and nickel-base stainless alloys that have achieved a significant neutron fluence in environments that span oxygenated to hydrogenated water at 270–340 °C. Because cracking susceptibility depends on many factors, such as alloy composition and microstructure, stress, radiation, and the environment, the failure mechanism has been termed irradiation-assisted stress corrosion cracking (IASCC). Initially, the affected components were either relatively small (bolts, springs, etc.) or those designed for replacement (fuel rods, control blades, or instrumentation tubes). Since these early observations, many more structural components (PWR baffle bolts and BWR core shrouds) have been identified to be susceptible to IASCC. Recent reviews [1, 2, 3, 4, 5] describe the current knowledge related to IASCC service experience and laboratory investigations and highlight the limited amount of well-controlled experimentation that exists on well-characterized materials.

The importance of neutron fluence on IASCC has been well-established (Fig. 15.1). Intergranular (IG) SCC is promoted in austenitic stainless steels as a critical *pseudo-threshold* fluence is exceeded. The dose to cracking is referred to as a *pseudo-threshold* because the value depends on the environmental and material parameters. Cracking is observed in BWR oxygenated water at fluences above about $2-5 \times 10^{20}\,\mathrm{n/cm^2}$ ($E > 1\,\mathrm{MeV}$), which corresponds to about 0.3–0.7 displacements per atom (dpa) (Fig. 15.2). While the fluence dependence on cracking is not strong, cracking does occur during ex situ, slow-strain-rate SCC testing of stainless steels irradiated in core. The occurrence of cracking in post-irradiation tests indicates that *persistent* radiation effects (material changes) are primarily responsible for IASCC susceptibility, although in situ effects like radiation creep relaxation of weld residual stresses and increased stress from differential swelling can be important. In fact, IASCC only occurs with the confluence of irradiation and an aggressive environment. If either is absent, cracking is either eliminated or greatly reduced.

IASCC can be categorized into radiation effects on (1) water chemistry (radiolysis), and (2) material properties, as summarized in Fig. 15.3. The cracking response to changes in water chemistry is similar for both irradiated and unirradiated materi-

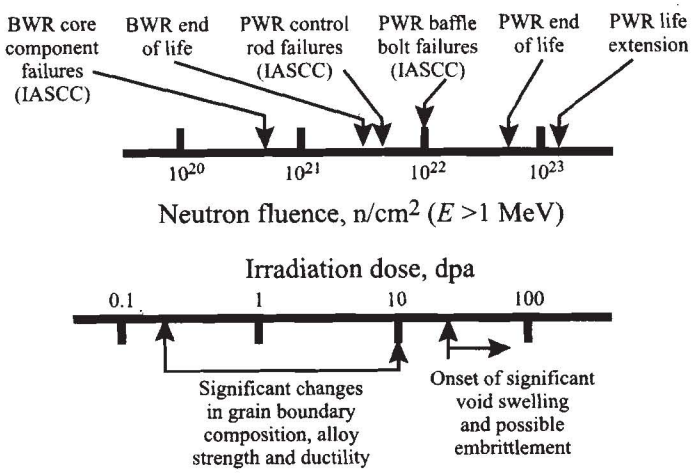


**Fig. 15.1.** Neutron fluence effects on irradiation-assisted stress corrosion cracking susceptibility of stainless steels in LWR environments (from [6])

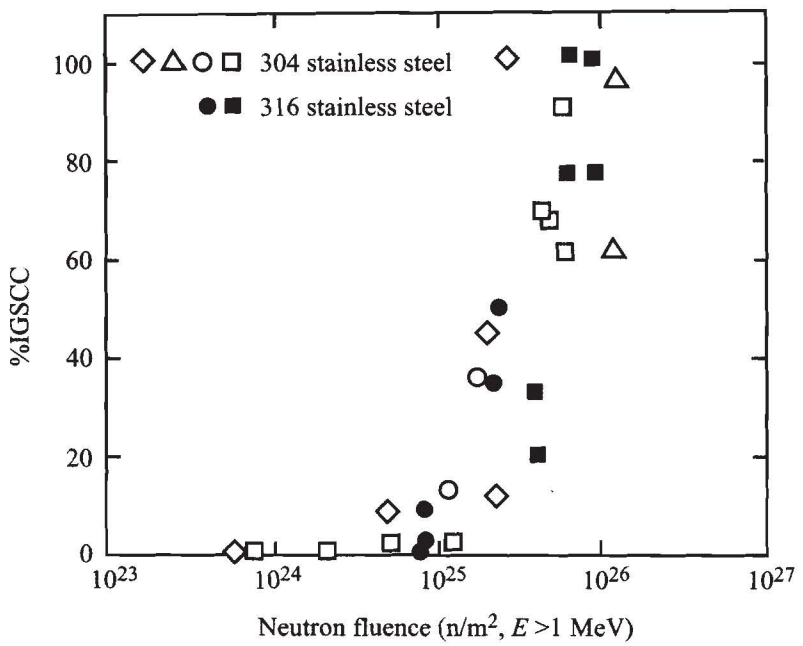


**Fig. 15.2.** Dependence of cracking in neutron-irradiated high-purity 304 SS and 316 SS on accumulated high-energy neutron fluence (from [4])

als. In both cases, there is a steep increase in environmental cracking kinetics with a rise in the corrosion potential above about $100mV_{SHE}$ [7, 8, 9]. At high corrosion potential, the crack growth rate also increases sharply as impurities (especially chlo-

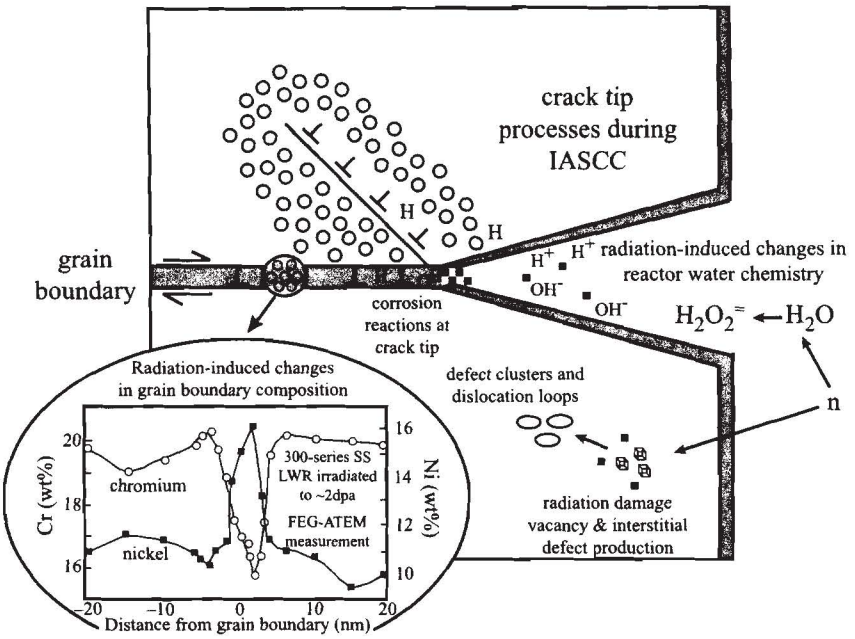


**Fig. 15.3.** Schematic illustration of mechanistic issues believed to influence crack advance during IASCC of austenitic stainless steels in LWRs (from [6])

ride and sulfate) are added to pure water in either the irradiated or unirradiated cases. In post-irradiation tests, the dominant radiation-related factors are microstructural and microchemical changes, which can be responsible for *threshold-like* behavior in much the same way as corrosion potential, impurities, degree of sensitization, stress, temperature, etc. Other radiation phenomena, like radiation creep relaxation and differential swelling, could also have *persistent* effects if the sources of stress present during radiation (e.g., weld residual stresses, or loading from differential swelling) were also present during post-irradiation testing. The effects of radiation rapidly (in seconds) achieve a dynamic equilibrium in water, primarily because of the high mobility of species in water. In metals, dynamic equilibrium is achieved only after many dpa, typically requiring years of exposure. As both radiation-induced segregation (RIS) of major elements, and radiation hardening (RH) and the associated microstructural development asymptotically approach a dynamic equilibrium, other factors (e.g., RIS of Si, or precipitate formation or dissolution) may become important. Data on post-irradiation slow strain rate tests (SSRT) on stainless steels show that there is a distinct (although not invariant) threshold fluence at which IASCC is observed under LWR conditions [8]. The term "threshold" is used here to characterize the regime where cracking increases steeply with fluence, but it does not mean that cracking is absent below the threshold or that cracking saturates at the threshold. Because this threshold occurs at a fraction to several dpa (depending on the alloy, stress, water chemistry, etc.), Fig. 15.2, in situ effects (corrosion potential,

## 15.3 Service and Laboratory Observations of Irradiation Effects on SCC

### 15.3.1 Austenitic Alloys

A historical perspective of IASCC service experience is instructive, as the phenomenon extends back to the 1960s, and the early observations and conclusions projected an accurate image of the important characteristics, generic nature, and broad relevance to plant components. As with other instances of environmental cracking, occasional early observations pointed the way toward a growing incidence with time and neutron fluence. IASCC was first reported in the early 1960s [1, 7, 20] and involved intergranular cracking of stainless steel fuel cladding. The findings and conclusions were that intergranular cracking morphology predominated, with initiation of multiple cracks occurring from the waterside. By contrast, only ductile, transgranular cracking was observed in post-irradiation mechanical tests performed in inert environments and at various temperatures and strain rates. Grain boundary carbide precipitation was generally not observed by optical or transmission electron microscopy (although pre-existing thermal sensitization was present in some cases). A correlation between time-to-failure and stress level was reported, with failure occurring first in thin-walled rods with small fuel-to-cladding gaps, where swelling strains were largest. The highest incidence of cracking occurred in peak heat flux regions, corresponding to the highest fluence and the greatest fuel-cladding interaction (highest stresses and strains). Similar stainless steel cladding in PWR service exhibited fewer instances of intergranular failure. At that time the PWR failures were attributed to off-chemistry conditions or stress rupture.

IASCC has since been observed in a growing number of other stainless steel (and nickel alloy) core components, such as neutron source holders in 1976 and control rod absorber tubes in 1978 [1]. Instrument dry tubes and control blade handles and sheaths, which are subject to very low stresses also cracked, although generally in creviced locations and at higher fluences [5]. Following an initial trickle of failures in the most susceptible components, numerous incidents of IASCC have been observed since the early 1990s, perhaps most notably in BWR core shrouds [1, 7, 20, 29] and PWR baffle bolts [34, 35].

Table 15.2 presents a broad summary of reported failures of reactor internal components, showing that IASCC is not confined to a particular reactor design. For example, stainless steel fuel cladding failures were reported in early commercial PWRs and in PWR test reactors. At the West Milton PWR test loop, intergranular failure of vacuum annealed type 304 stainless steel fuel cladding was observed in 316 °C ammoniated water (pH 10) when the cladding was stressed above yield. Similarly, IASCC was observed in creviced stainless steel fuel element ferrules in the Winfrith SGHWR, a 100 MWe plant in which light water is boiled within pressure tubes, giving rise to a coolant chemistry similar to other boiling water reactor designs.

Reactor type comparisons were also made in swelling tube tests performed in the core of a BWR and a PWR on a variety of commercial and high purity heats of

**Table 15.2.** IASCC service experience (after [5])

| Component | Alloy | Reactor type | Possible sources of stress |
|---|---|---|---|
| Fuel cladding | 304 SS | BWR | Fuel swelling |
| Fuel cladding | 304 SS | PWR | Fuel swelling |
| Fuel cladding* | 20%Cr/25%Ni/Nb | AGR | Fuel swelling |
| Fuel cladding ferrules | 20%Cr/25%Ni/Nb | SGHWR | Fabrication |
| Neutron source holders | 304 SS | BWR | Welding & Be swelling |
| Instrument dry tubes | 304 SS | BWR | Fabrication |
| Control rod absorber tubes | 304/304L/316L SS | BWR | $B_4C$ swelling |
| Fuel bundle cap screws | 304 SS | BWR | Fabrication |
| Control rod follower rivets | 304 SS | BWR | Fabrication |
| Control blade handle | 304 SS | BWR | Low stress |
| Control blade sheath | 304 SS | BWR | Low stress |
| Control blades | 304 SS | PWR | Low stress |
| Plate type control blade | 304 SS | BWR | Low stress |
| Various bolts** | A-286 | PWR & BWR | Service |
| Steam separator dryer bolts** | A-286 | BWR | Service |
| Shroud head bolts** | 600 | BWR | Service |
| Various bolts | X-750 | BWR & PWR | Service |
| Guide tube support pins | X-750 | PWR | Service |
| Jet pump beams | X-750 | BWR | Service |
| Various springs | X-750 | BWR & PWR | Service |
| Various springs | 718 | PWR | Service |
| Baffle former bolts | 316 SS Cold-work | PWR | Torque, differential swelling |
| Core shroud | 304/316/347 /L SS | BWR | Weld residual stress |
| Top guide | 304 SS | BWR | Low stress (bending) |

* Cracking in AGR fuel occurred during storage in spent fuel pool

** Cracking of core internals occurred away from high neutron and gamma fluxes

types 304, 316 and 348 stainless steel and Alloys X-750, 718 and 625. Swelling was controlled by varying the mix of $Al_2O_3$ and $B_4C$ within the tubes; the latter swells as neutrons transmute B to He. Nominally identical strings of specimens were inserted into the core in place of fuel rods. The distinction in the IASCC response between the two reactor types was small. While the available data clearly support a linkage between IASCC in BWRs and PWRs, it is clear that the elevated corrosion potential in BWRs accelerates SCC, and to a lesser extent, the generally higher flux and temperature in PWRs also accelerates SCC.

Laboratory data support that obtained in the plant in terms of the accelerating effect of irradiation. Since laboratory data is collected post-irradiation in which radiolysis of the water is not a factor, the effects of irradiation that are responsible for the observed cracking is deduced to come from changes in the microstructure. Figure 15.32 shows the effect of irradiation on the crack growth rate of 304 and 316 stainless steel under continuous cycling in 289 °C high purity water with ~ 300 ppb dissolved oxygen as compared to that in air. The 45° line indicates no effect of the environment on cracking and the two curves represent the expected crack growth rates for unirradiated austenitic stainless steels in high-purity water

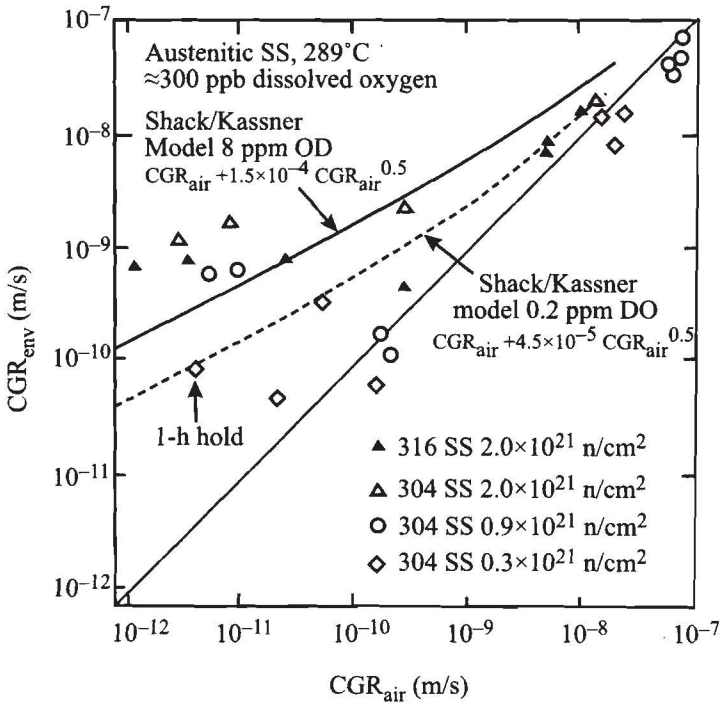


**Fig. 15.32.** Comparison of the crack growth rate in irradiated austenitic stainless steels under continuous cycling in 288 °C high purity water containing 300 ppb $O_2$ compared to that in air (from [36])

with either 8 ppm (solid) or 0.2 ppm (dashed) dissolved oxygen [36]. By comparing the data at different neutron fluence levels, it is clear that both the environment and the fluence level affect the crack growth rate. The crack growth rate in 304 SS irradiated to $2 \times 10^{21}\,n/cm^2$ is over an order of magnitude greater than that for irradiation at $0.3 \times 10^{21}\,n/cm^2$.

Since the early 1990s, the plant and laboratory evidence of IASCC makes a compelling case that cracking is environmentally assisted and that there is a well-behaved continuum in response over ranges in fluence, corrosion potential, temperature, stress, etc. Since there is a consistent trend toward increasing IASCC susceptibility with increasing corrosion potential in BWRs (e.g., Figs. 15.30a and 15.31), PWRs should be less susceptible to IASCC. However, other factors distinguish PWRs from BWRs, including their higher temperatures, $\approx 10\times$ higher neutron fluence in core structural components, higher hydrogen fugacity, and the borated-lithiated water chemistry (including the possibility of localized boiling and thermal concentration cells in crevices from gamma heating which could lead to aggressive local chemistries). The possible role of radiation-induced segregation of Si may be especially important in accounting for the limited difference in SCC response at high potential (BWR) vs. low potential (PWR) at high fluence.

The two most widespread examples of irradiation-assisted SCC are in BWR core shrouds and PWR baffled bolts although susceptibility clearly exists in other areas, such as control blade components, fuel components, the BWR top guide, etc., SCC in the BWR core shroud occurs almost exclusively near the welds (both circumferential and vertical), and initiation is observed from both the inside (ID) and outside (OD) surfaces (the shroud separates the upward core flow from the downward re-circulation flow that occurs in the annulus between the shroud and the pressure vessel). This large diameter welded "pipe" has inherent susceptibility to SCC, related primarily to weld residual stresses and weld shrinkage strains, and cracking is observed in both low fluence and moderate fluence areas. Severe surface working has also been found to aggravate IASCC in core shrouds. The extent of the enhancement in SCC susceptibility by irradiation is limited, because while radiation hardening and radiation-induced segregation occur, radiation creep relaxes the weld residuals stress.

Extensive failures of PWR baffle bolts have occurred beginning in the 1990s [34, 35] although large plant-to-plant and heat-to-heat differences are observed. Most baffle bolts are fabricated from type 316 stainless steel cold-worked to $\approx 15\%$ to increase their yield strength. The complex baffle former structure exists in a PWR because the fuel does not have a surrounding "channel", so the baffle former structure must conform closely to the geometry of the fuel to provide well-distributed water flow. The baffle former plates are usually made from annealed type 304 stainless steel. Because of their proximity to the fuel, very high fluences can develop, up to $\sim 80$ dpa by the end of the original design life. The high gamma flux produces significant heating in the components, in some instances estimated at 40 °C above the coolant temperature, especially in designs where the PWR coolant does not have good access to the bolt shank. Figure 15.33 shows micrographs of IG cracking in

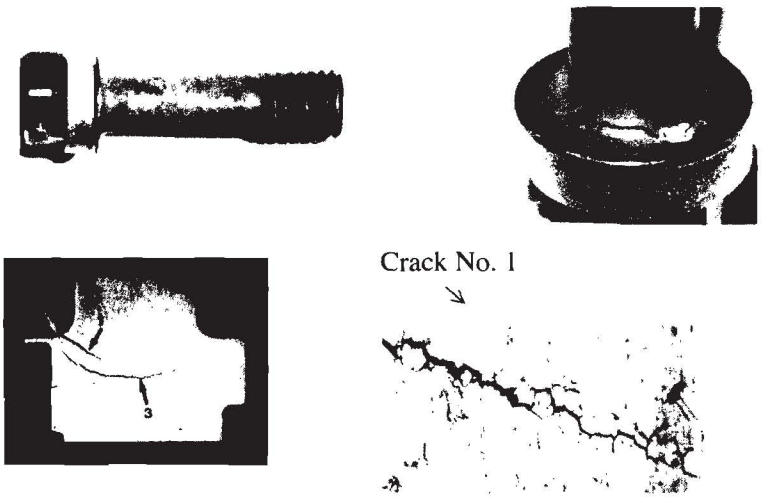


**Fig. 15.33.** Cracks in cold-worked 316 stainless steel baffle bolt. The location of the cracks received a neutron dose of about 7 dpa at $\sim 310\,^{\circ}\mathrm{C}$ (courtesy, Electrabel)

the baffle bolt described earlier in Chap. 8 on swelling. Note that the cracks are occurring where the shank meets the head. Cracks are completely intergranular and penetrate greater than half the thickness of the bolt.

The number of IASCC incidents has continued to grow as more and more components in LWRs are revealed to be susceptible. The overall trends and correlations for IASCC can be summarized as follows:

- While intergranular cracks related to radiation effects in solution annealed stainless steel were once thought to occur only at fluences above $\approx 0.3 \times 10^{21}\,\mathrm{n/cm^2}$, significant intergranular cracking in BWR core shrouds over a broad range of fluences make it clear that such a distinction (a true fluence threshold) is not justified. Of course, observations of SCC in unsensitized stainless steel (with or without cold-work) also render untenable the concept of a threshold fluence, below which no SCC occurs. This also holds for thresholds in corrosion potential, water impurities, etc.
- Fluence affects SCC susceptibility, but almost always in a complex fashion. SCC in BWR shrouds and PWR baffle bolts does not always correlate strongly with fluence, one important reason for this is that radiation creep produces relaxation of the stresses from welding and in bolts.
- High stresses or dynamic strains were involved in most early incidents; however, cracking has been observed at quite low stresses at high fluences and longer operating exposure. Laboratory and field data indicate that IASCC occurs at stresses below 20% of the irradiated yield stress, and at stress intensities below $10\,\mathrm{MPa\,m^{1/2}}$.
- A strong effect of corrosion potential is clear from extensive laboratory and field data. Its effect is generally consistent from low to high fluence, although the

quantitative change associated with changes in potential vary. Materials prone to high radiation-induced changes in Si level may exhibit a very limited effect of corrosion potential. A true threshold potential clearly does not exist, as irradiated materials exhibit IASCC in de-aerated water.

- Solution conductivity (i.e., impurities, especially chloride and sulfate) strongly affects cracking propensity in BWR water. This correlation applies equally to low and high flux regions and to stainless steels and nickel-base alloys. Indeed, the correlation closely parallels that from out-of-core.
- Crevice geometries exacerbate cracking due primarily to their ability to create a more aggressive crevice chemistry from the gradient in corrosion potential (in BWRs) or in temperature (most relevant to PWRs).
- Cold-work often exacerbates cracking (esp. abusive surface grinding), although it can also delay the onset of some radiation effects.
- Temperature has an important effect on IASCC, enhancing both crack initiation and growth rate.
- Grain boundary carbides and chromium depletion are not required for susceptibility, although furnace sensitized stainless steels are clearly highly susceptible to cracking in-core. Cr depletion remains a primary culprit, although its effect is most pronounced in pH-shifted environments, as can develop when potential or thermal gradients exist. The role of N, S, P, and other grain boundary segregants is less clear.
- The fluence at which IASCC is observed is dependent on applied stress and strain, corrosion potential, solution conductivity, crevice geometry, etc. At sufficiently high conductivities, cracking has been observed in solution annealed stainless steel in the field and in the laboratory. Thus, while convenient in a practical engineering sense, the concept of a "threshold" fluence (or stress, corrosion potential, etc.) is scientifically misleading as cracking susceptibility and morphology are properly considered an interdependent continuum over many relevant parameters.

The field and laboratory data available in the early 1980s, coupled with broader fundamental understanding of environmental cracking in hot water, led to the hypothesis that among innumerable possible radiation effects the most significant factors were radiation-induced segregation at grain boundaries, radiation hardening (elevation of the yield strength), deformation mode, radiation creep relaxation (of constant displacement stresses, e.g., in welds and bolts), and radiolysis (elevated corrosion potential in BWRs). Other factors could also be important in some instances, such as void formation, which may also affect fracture toughness, and can produce differential swelling that causes re-loading of components like baffle bolts.

### 15.3.2 Ferritic Alloys

Ferritic alloys are also susceptible to environmentally enhanced cracking in high-temperature water. The role of irradiation alone on the fatigue crack growth rate in pressure vessel steels was discussed in Chap. 13, where it was determined that

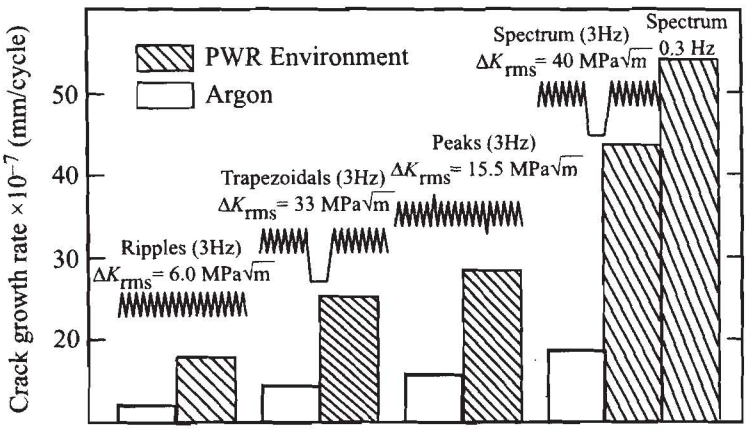


**Fig. 15.34.** The effect of environment, frequency and transients on the fatigue crack growth behavior of A533B steel subjected to various loading sequences (from [37])

irradiation alone did not accelerate crack growth rate. However, crack growth rates *are* affected by the environment. In fact, the environment, loading parameters and material parameters all affect the crack growth rate in high-temperature water. In general, crack growth per cycle increases with:

Environmental parameters
- Increased oxygen concentration
- Increased conductivity
- Increased temperature

Loading parameters
- Increased $R$ ratio (higher mean stress)
- Decreasing frequency
- Transients and hold periods in the waveform

Material parameters
- Increasing sulfur content in the alloy

For example, Fig. 15.34 shows the effect of environment, frequency and load waveforms on the fatigue crack growth rate in A508 steel. In a PWR environment, lower frequency, transients and hold times in the waveforms increase the crack growth rate. The effect of the environment on cracking is shown in Fig. 15.35a, which gives the fatigue crack growth rate as a function of $\Delta K$ for A533B steels and welds in PWR water. The solid line at right is the ASME Boiler and Pressure Vessel Code bounding crack growth rate in air. As is evident, the environment has a significant effect on both the growth rate and the dependence of $da/dN$ on $\Delta K$. Figure 15.35b also shows that in reactor grade water at 288 °C, the effect of irradiation only minimally augments the crack growth rate due to the environment.

Gary S. Was

**Fundamentals of Radiation Materials Science**

Metals and Alloys

Radiation Materials Science teaches readers the fundamentals of the effects of radiation on metals and alloys. When energetic particles strike a solid, numerous processes occur that can change the physical and mechanical properties of the material. Metals and alloys represent an important class of materials that, by virtue of their use in nuclear reactor cores, are subject to intense radiation fields. Radiation causes metals and alloys to swell, distort, blister, harden, soften and deform. This textbook and reference covers the basics of particle-atom interaction for a range of particle types, the amount and spatial extent of the resulting radiation damage, the physical effects of irradiation and the changes in mechanical behavior of irradiated metals and alloys. Concepts are developed systematically and quantitatively, supported by examples, references for further reading and problems at the end of each chapter. Beyond addressing students enrolling for a materials sciences or nuclear engineering degree, the book will benefit professionals in laboratories, reactor manufacturers and specialists working in the utility industry.

ISBN 978-3-540-49471-3

9 783540 494713

springer.com